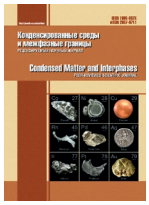

ISSN 1606-867X (Print)
ISSN 2687-0711 (Online)
Condensed Matter and Interphases
Kondensirovannye Sredy i Mezhfaznye Granitsy
https://journals.vsu.ru/kcmf/

Original articles

Research article
https://doi.org/10.17308/kcmf.2022.24/10553

Mathematical modelling of vortex structures in the channel of an electrodialysis cell with ion-exchange membranes of different surface morphology

K. A. Lebedev[1]✉, V. I. Zabolotsky[1], V. I. Vasil'eva[2], E. M. Akberova[2]

[1]Kuban State University,
149 Stavropolskaya ul., Krasnodar 350040, Russian Federation

[2]Voronezh State University,
1 Universitetskaya pl., Voronezh 394018, Russian Federation

Abstract

One of the ways to obtain membranes with electroconvection as the dominant mechanism of ion transport is to optimise the surface of known brands of commercial heterogeneous membranes by changing their manufacturing technology. For example, the degree of dispersion of the ion-exchanger or the volume ratio of the ion-exchanger to inert binder can be changed. The aim of this study was to determine and theoretically analyse the fundamental correlations between the intensity of electroconvection and the surface morphology of ion-exchange membranes with different ion-exchanger particle content.

The article presents a mathematical model of ion transport across the ion-exchange membrane/solution interface in the channel of an electrodialysis cell. The phenomenon of electroconvection in electromembrane systems (EMS) was modelled by solving two-dimensional Navier-Stokes equations for an incompressible liquid with no-slip boundary conditions and a set distribution of the electric body force. The body force distribution was set taking into account the real size of ion-exchanger particles and the distance between them that determine the electrical heterogeneity of the surface of experimental ion-exchange membranes with different mass fractions of ion-exchange resin.

It was determined that in the numerical modelling, the most important parameters were the size of the sections of electrical heterogeneity of the membrane surface, the current density, and the length of the space charge region (SCR). Numerical calculations were presented to determine the vortex size depending on the current density and the degree of electrical heterogeneity of the membrane surface.

It was shown that an increase in the mass fraction of ion-exchange resin in the production of heterogeneous sulphocation-exchange membranes resulted in a decrease in the step of electrical surface heterogeneity and promoted the formation of electroconvective vortices interacting with each other. Within the boundary conditions and approximations of the mathematical model, the vortex sizes reach their maximum value in the middle of the heterogeneity section L_0.

Keywords: Mathematical modelling, Electroconvection, Vortex structures, Heterogeneous ion-exchange membrane, Surface morphology, Electrical heterogeneity of surface

Funding: The study was supported by a grant from the Russian Science Foundation No. 21-19-00397, https://rscf.ru/en/project/21-19-00397/

For citation: Lebedev K. A., Zabolotsky V. I., Vasil'eva V. I., Akberova E. M. Mathematical modelling of vortex structures in the channel of an electrodialysis cell with ion-exchange membranes of different surface morphology. *Condensed Matter and Interphases*. 2022;24(4): 483–495. https://doi.org/10.17308/kcmf.2022.24/10553

Для цитирования: Лебедев К. А., Заболоцкий В. И., Васильева В. И., Акберова Э. М. Математическое моделирование вихревых структур в канале электродиализной ячейки с ионообменными мембранами разной морфологии поверхности. *Конденсированные среды и межфазные границы*. 2022;24(4): 483–495. https://doi.org/10.17308/kcmf.2022.24/10553

✉ Konstantin A. Lebedev, e-mail: klebedev.ya@yandex.ru

1. Introduction

One of the current goals of membrane electrochemistry and electromembrane technology is to enhance the mass transfer of electrolyte ions through ion exchange membranes. In EMS with a conventional electrodiffusion ion transport mechanism, the velocity of the process is limited by the value of the limiting electrodiffusion current. Hydrodynamic techniques are widely used to increase the value, such as increasing the flow velocity of the solution, using turbulent inserts and/or a mixed layer of ion exchangers, and profiling the membrane surface.

Another approach to the intensification of electromembrane processes is based on the use of new mechanisms of ion delivery to the membrane surface. Under intensive current modes, electroconvection is the dominant mechanism [1–6]. In such cases, the velocity of the process involving heterogeneous membranes with an electrically heterogeneous surface may exceed the velocity of transfer across homogeneous membranes. This aspect is important because foreign-made homogeneous membranes are several times more expensive than heterogeneous membranes. Key factors in the development of electroconvection are the chemical nature of the functional groups and polymer matrix and the morphology of the membrane surface. The surface morphology depends on the distribution of conductive sections of the ion-exchanger and inert sections of the polyethylene binder, as well as their size.

The basic principles of electroconvection are described in works by Dukhin and Mishchuk [3, 4], Rubinstein et al. [4–7]. Studies [8–10] describe the possibility of enhancing mass transfer in EMS by improving the surface morphology of ion-exchange membranes. The use of membranes with optimised surface morphology in electrodialysis for desalting and deionisation of natural waters and technological solutions provides the prerequisites for a significant increase in efficiency of these processes in overlimiting current modes. The transport characteristics of ion-exchange membranes depend on the degree of electrical (alternation of conductive and non-conductive surface sections) and geometrical (microrelief) heterogeneity of their surface [1, 2]. The results of mathematical modelling showed that alternating conductive and non-conductive sections on the surface of heterogeneous membranes can ensure the occurrence of electroconvective flows at significantly smaller jumps of electric potential in comparison to homogeneous membranes.

The aim of this study was to determine and theoretically analyse the fundamental correlations between the intensity of electroconvection and the surface morphology of ion-exchange membranes with different ion-exchanger particle content.

2. Theoretical analysis

2.1. Theory of electroconvection in electromembrane systems

A characteristic feature of electrodialysis in overlimiting current modes is that the electric field induces a body force, which stimulates the movement of both ions and the volume of the solution. This phenomenon is called electroconvection. It manifests as microscopic hydrodynamic phenomena (even at the Reynolds number $Re = 0$), which have the properties of regular turbulence at high values of Re. The influence of any non-hydrodynamic processes on the solution flow is carried out through the body force in the Navier–Stokes equation [11, 12]. Electroconvection is caused by the vortex nature of the body force ($rot\vec{f} \neq 0$). In the case of EMS, the volumetric force is the electric force acting on the space charge: $\vec{f} = \rho\vec{E}$ where ρ is the charge distribution density and E is the electric field intensity. Electroconvection in EMS with homogeneous ion-exchange membranes is determined by a counterion concentration gradient, which is caused by uneven desalting of the solution along the length of the channel of the electrodialysis unit [13]. Due to the difference in charge numbers and diffusion coefficients of cations and anions, values of $\vec{f}$ near the anion-exchange and cation-exchange membranes are different. Consequently, the solution flow in the channel is asymmetrical. This mechanism of electroconvection has been theoretically studied by Rubinstein et al. [5–7]. Electroconvection has a threshold character and appears when a certain critical value of electric potential drop is reached.

In EMS with heterogeneous membranes, the electroconvection mechanism is different. Heterogeneous membranes are produced by hot

pressing or rolling dispersed ion-exchange resins with a particle size of 10 to 100 μm and an inert polyethylene binder. The structure and surface of heterogeneous membranes are inhomogeneous. On the membrane surface, there is an alternation of the active conductive sections (ion exchanger particles) and inert non-conductive sections of polyethylene. The proportion of active surface depends on the membrane production technology. At overlimiting current densities, an electric vortex force arises in the system, resulting in the occurrence of electroconvective vortices. In [3, 4], it was shown that this mechanism has no threshold value of potential drop. It occurs at significantly lower values of electric current density than in the homogeneous membrane systems. Enhanced ion transport may depend on the surface morphology of ion-selective membranes as well as the heterogeneity of their electrochemical properties.

In contrast to conventional turbulence, which has been extensively studied theoretically and experimentally for many decades, the phenomenon of electroconvective turbulence has just undergone the initial basic numerical experiments. The current aim is to provide the resultant mathematical statements that adequately describe the experimental data.

2.2. Mathematical modelling of electroconvective vortex structures in the channel of an electrodialysis unit for membranes with two conductive sections

Studies [1, 6] set the goal to theoretically investigate the regularities of electroconvection in a smooth rectangular desalting channel of an electrodialysis unit with heterogeneous ion-exchange membranes. The two-dimensional mathematical model describing the processes during operation of the electrodialysis cell in overlimiting current modes is based on the Navier-Stokes equations written in terms of the continuity condition for a steady-state mode [6]:

$$(u\cdot\nabla)u=\nabla\cdot\left(-\frac{1}{\rho}p+\nu(\nabla\cdot u)\right)+\frac{1}{\rho}\bar{f}(x,y), \quad (1)$$

$$(\nabla\cdot u)=0, \quad (2)$$

where u is the velocity vector, $\bar{f}(x,y)$ is the body force acting in the space charge region (SCR) (N/m^3), ρ is the solution density (1000 kg/m^3), $\nu=10^{-6}$ m^2/s is the dynamic viscosity, $\mathrm{Re}_y=\frac{V_{\max}H}{\nu}$ is the Reynolds number, $V_{\max}$ is the longitudinal maximum velocity of solution flow in the electrodialysis cell, p is the pressure; and H is the intermembrane distance.

When formulating the boundary conditions, it was assumed that the velocity profile at the inlet of the membrane channel was parabolic (laminar flow). No-slip conditions were applied to the membrane surface. At the outlet of the channel, the hydrostatic pressure was zero:

$$y=0, u=u_{\max}x\left(l-\frac{x}{h}\right);\ \ x=0, u=0;$$

$$y=L, p=0;\ \ x=H, u=0. \quad (3)$$

To solve equations (1) – (3), it is necessary to know the distribution of the body force $\vec{f}(x,y)$, arising under the effect of the electric field on the volumetric space charge near the interfaces in the channel. Figure 1 shows a schematic of the membrane surface (Fig. 1a), the distribution profile of the electric force acting over the membrane sections with different values of electrical conductivity (Fig. 1b), and the position of the membrane in the electrodialysis channel (Fig. 1c). We identified conductive and non-conductive sections on the surface of heterogeneous membranes, as well as a transition section of about 0.1 μm. Consequently, the body force $\vec{f}$ was specified in the regions of the electroneutrality violation zone S_2, adjacent to the boundaries of $x=0$, $x=H=2$ mm (Fig. 1c). According to Rubinstein's theory [5], the space charge extent λ at its limit can approach the thickness of the diffusion layer. In paper [1], it was assumed to be $\lambda=2$ μm. In this study, the value of λ was assumed to depend on the current density $\lambda=\left(1-\frac{i_{\lim}}{i}\right)\delta$, where δ is the thickness of the diffusion layer. Under the condition of $i=i^0_{\lim}$, the value of space charge region (SCR) is zero. As the current increases, the value of λ approaches the value of the diffusion layer thickness. If we build models using atomic force microscopy data [13], the thickness of the SCR can be in the range of 200–1200 nm [14] or even less than 50–100 nm. The size of the SCR is quite

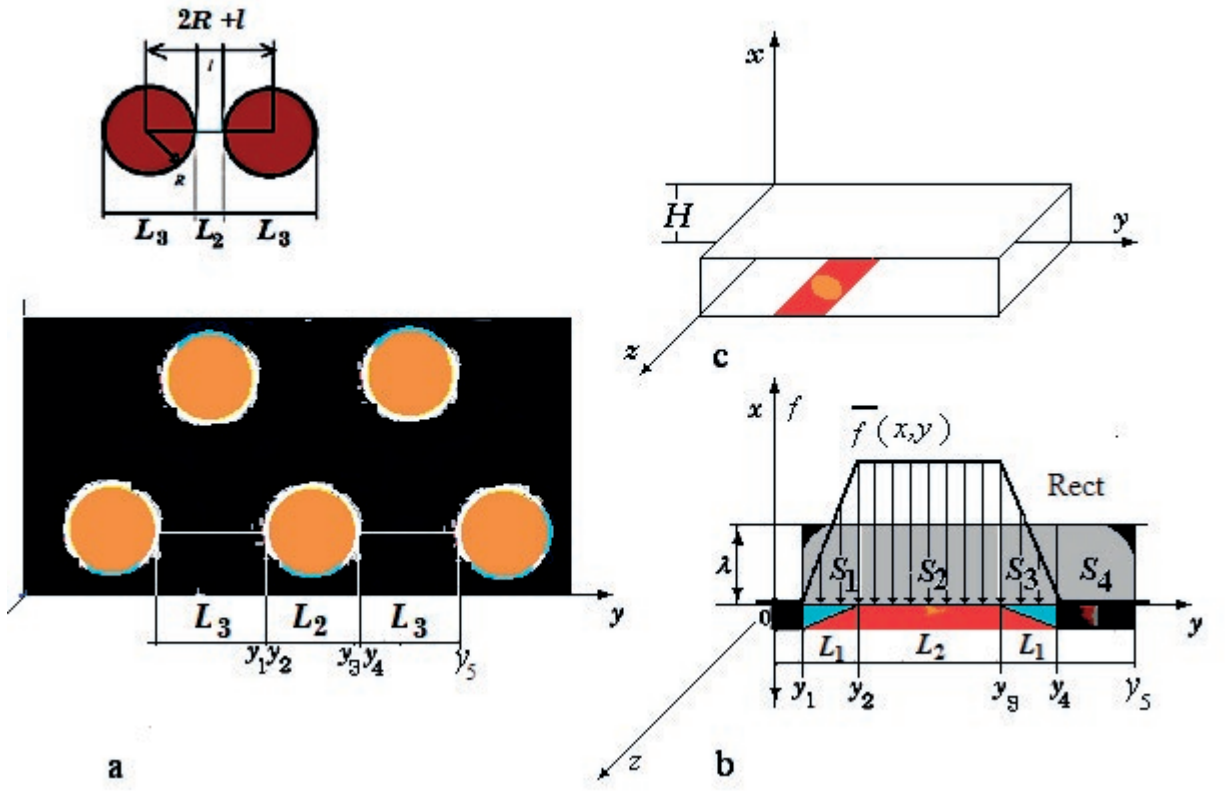

Fig. 1. Schematic representation of the model membrane surface in the electrodialysis cell (a): the circles are conductive sections of the ion exchanger L_2, the dark field is the non-conductive sections of the polyethylene L_3, and the boundary is the transition sections L_1. Electric force distribution profile (b) acting on S_1, S_2, S_3, S_4: $S_1 = \{(x,y): y_1 \le y \le y_2, 0 \le x \le \lambda\}$, $S_2 = \{(x,y): y_3 \le y \le y_4, 0 \le x \le \lambda\}$, $S_3 = \{(x,y): y_2 \le y \le y_3, 0 \le x \le \lambda\}$, $S_4 = \{(x,y): y_4 \le y \le y_5, 0 \le x \le \lambda\}$ with characteristic size values of L_1, L_2, L_3, respectively; λ is the thickness of the SCR. Rect indicates the rectangle corresponding to the conductive sections of the membrane, consisting of the combined rectangles S_1, S_2, S_3 with a height of λ and a width of $2L_3 + L_2$

difficult to determine, it requires many factors to be taken into account.

In this study, we first coordinated the data in Rubinstein's model and in the works of other authors [15], who considered the space charge to be the main driving force of electroconvection [16–20]. The height of the trapezoid $f_{\max}$ (Fig. 1b) is the maximum of the space charge distribution function, which corresponds to its value at the membrane surface. It is calculated by formula (5). The electric body force $\vec{f}_x = \rho_e E_x$ (N/m^3) is determined by the electric charge density ρ_e and the electric field strength E. A force vector field arises as a result of the electric field in a SCR with a thickness of λ. The y-axis component of the force is zero $\vec{f}_y(x,y) = 0$. Similarly to studies [1, 10], we assumed that $\vec{f}$ varies piecewise-linearly along the longitudinal axis y: in section S_1, the force changes from 0 to $|f_{\max}|$, and in S_2 it decreases from $|f_{max}|$ to 0. In section S_3, the force is constant and equal to $f = f_{max}$. In the non-conductive section S_4, the electric force is zero. Therefore,

$$f(x,y) = \begin{cases} \dfrac{y - y_1}{y_2 - y_1} f_{\max}; (x,y) \in S_1 \\ f_{\max}; (x,y) \in S_2 \\ \dfrac{y - y_4}{y_3 - y_4} f_{\max}; (x,y) \in S_3 \\ 0; (x,y) \in S_4, \end{cases} \quad (4)$$

In [1], the relationship between the body force and the current density was determined:

$$f_{\max} = Fc_1 E = \frac{RT}{D_1 F} i = k_f i, \quad (5)$$

where $k_f = 2.5 \cdot 10^7$ has the dimension of N/(m·A), if the current density is expressed in [A/m^2]. This

force acts at each point of the SCR, which is formed in a rectangle with a length of L_2 and a width of λ, where $\lambda = \left(1 - \frac{i^0_{\text{lim}}}{i}\right)\delta$ is the thickness of the SCR and δ is the thickness of the diffusion layer. The electric force is directed along the normal to the membrane (coaxial to the spatial coordinate *x*). The coordinates of the electrodialysis cell (c) are: *y* – length, $0 \le y \le L$; *x* – height, $0 \le x \le H$; *H* – intermembrane distance, *z* – width of the electrodialysis cell.

In [10], two cases of the surface morphology of ion-exchange membranes with a geometric heterogeneity step of $2R+l$ were considered: 1) $2R + l = 2{\cdot}30 + 70 = 130$ μm, $2R/l = 60/70 = 0.875$; 2) $2R + l = 2{\cdot}50 + 30 = 130$ μm, $2R/l = 100/30 = 3.34$, for the channel length $L = 130$ and its width of 400 μm. In our study, we used the surface characteristics of the experimental sulphocation-exchange membranes with different ion-exchange resin contents (Table 1) and, correspondingly, with different surface parameters: 1) $2R + l = 9.3$ μm, $2R/l = 0.89$; 2) $2R + l = 8.2$ μm, $2R/l = 1.05$ at the channel length $L = 6.2$; 3) $2R + l = 7.1$ μm, $2R/l = 1.84$ at the channel length $L = 7.1$ and its width of 2000 μm. Since we used the same grinding of the ion exchange resin for the experimental membrane samples, all the samples had approximately the same radius of ion exchange particles *R*.

2.3. Mathematical description of the membrane/solution interface, considering the microrelief

In theoretical works describing the regularities of the transmembrane electrodiffusion ion transport, the model of a homogeneous membrane with a flat boundary is usually used. However, direct experiments on the surface profile of the membrane by AFM (Fig. 2) showed that the transition boundary from the solution phase to the solid phase of the membrane cannot be modelled correctly by an ideal plane. The electrical properties of the boundary with a microprofile depend on the distribution of the local exchange capacity $Q(x)$ of the membrane within the specified spatial limits. The approximation of the distribution of the averaged exchange capacity along the normal to the membrane surface $Q(x) = q(x)Q_0$ was one of the problems in the mathematical description of the ion transport along a rough surface. Figure 2 shows an example of obtaining $q(x)$. Digital techniques of atomic force microscopy were applied to obtain the cross-sectional area of the solid phase $S(x)$, the microprofile was partitioned by height at different distances. We assumed that the solid phase fraction is $q(x) = S(x)/S_0$, where S_0 is the area of the experimentally studied membrane section. The cross-sections of the sulphocation-exchange membrane microprofile were numbered from 0 to 7. For each cross-section, the solid phase fraction is calculated as the ratio of the total area of the blackened areas *S* along the cross-section of the membrane microprofile (projected on the membrane surface) to the total area of the experimentally studied membrane sample S_0. The calculated area has a size of $S_0 = 12\times12\times10^{-12}$ m^2. The horizontal scale in Fig. 2 is 1000 times larger than the vertical scale. The proportion of the ion exchanger in cross-section *4* is defined as $\frac{Q}{Q_0} \approx q(x) = \frac{S}{S_0} = \frac{S2+S4}{S1+S2+S3+S4+S5}$. As the cross-section number increases, the solid phase fraction $q(x) = Q/Q_0$ increases. This results in dependence of the exchange capacity $Q(x)$ on *x*-coordinate (Table 2). The continuous distribution of the solid phase volume fraction

Table 1. Surface characteristics of experimental samples of swollen heterogeneous sulphocation-exchange membranes

Ion exchanger fraction, wt%	*S*, %	$\bar{r}$, μm	*P*, %	$\bar{r}$, μm	$\bar{l}$, μm	$2R+l$, μm	$2R/l$
45	21±1	2.2±0.1	1.9±0.1	1.9±0.1	4.9±0.4	9.3	0.89
55	25±2	2.1±0.1	2.2±0.3	1.9±0.2	4.0±0.3	8.2	1.05
70	38±2	2.30±0.04	3.2±0.4	1.9±0.1	2.5±0.1	7.1	1.84

S, % is the ion exchanger fraction; $\bar{r}$, μm is the weighted average radius of ion exchange sections; P, % is the macropore fraction; $\bar{r}$, μm is the weighted average pore radius; and $\bar{l}$, μm is the weighted average distance between the conductive regions

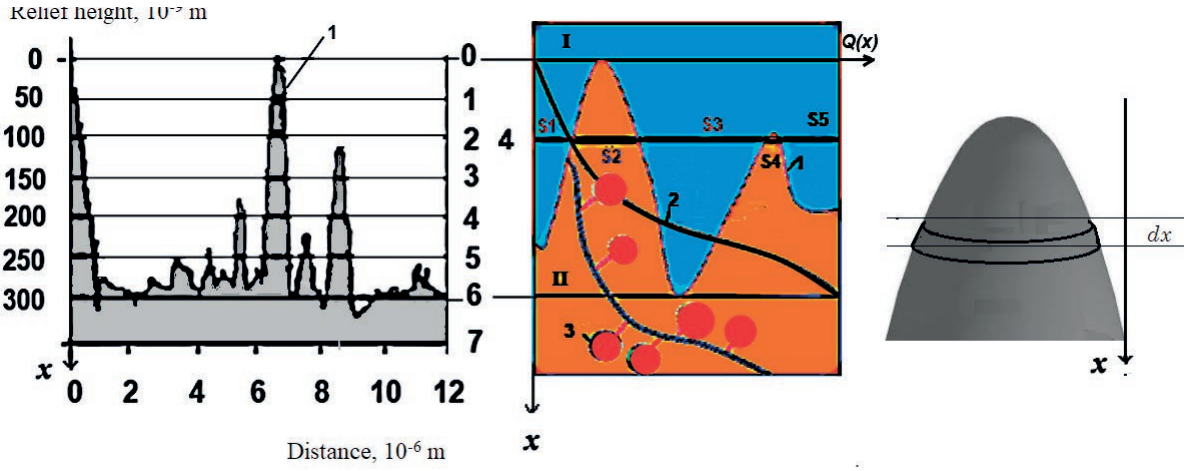

a b c

Fig. 2. Microprofile of the sulphocation-exchange membrane surface (a), the cross-sections in which the volume fraction of the solid phase was calculated (b), and a single microrelief section with a defined volume element of characteristic length *dx* (c). I – solution phase; II – membrane phase; *1* – surface microprofile; *2* – exchange capacity; *3* – ionogenic groups; and *4* – the cross-section used to determine the ionite content

Table 2. Volume fraction of the ion exchanger depending on the number of the layer cross-section

Cross-section	0	1	2	3	4	5	6	7
Volume fraction of the solid phase $q = Q/Q_0$	0	0.025	0.050	0.067	0.167	0.583	0.980	1.000

along the layer coordinate in the solution was obtained by interpolating using 3rd degree splines and 4th degree polynomials (Fig. 3).

We chose such a volume element so that it exceeded the size of the individual phases of the system. At the same time, it should be small enough to consider the dependence of the average volume concentration of ionogenic groups $q(x)$ and ionized groups on the side surface of the selected element as a function of the x-coordinate. The $q(x)$ dependence also takes into account, on average, the growth of the lateral area of the *dx* element, where the ionised groups involved in the splitting of water molecules are concentrated. In order not to complicate the theory with secondary dependencies, we assumed $q(x)$ to be the only primary characteristic that depends on the x-coordinate. The ion concentration c_j at a certain coordinate of x represents the average concentration of ions in the solid phase and in the solution phase. At $x = 0$, all ions are in the solution, and at $x = \delta$ they are in the solid phase.

Numerical calculations were carried out for micro-layer thickness between 1 and 300 nm. The exchange capacity distribution as a function of the dimensionless coordinate was assumed to be the same for all cases. Fig. 4 shows the change in the shape of the space charge and its integral value. The distribution of the space charge ρ over the layer thickness is determined

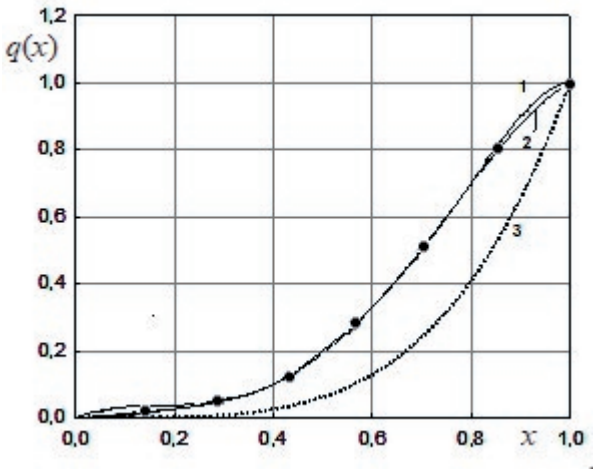

Fig. 3. Dependence of the solid phase volume fraction q on dimensionless layer thickness in the solution. *1* – interpolation of the data in Table 2 using splines; *2* – the polynomial approximation $q(x) = -4.45x^4 + 8.28x^3 - 3.397x^2 + 0.569x$; and 3 – the function of $q(x) = x^4$

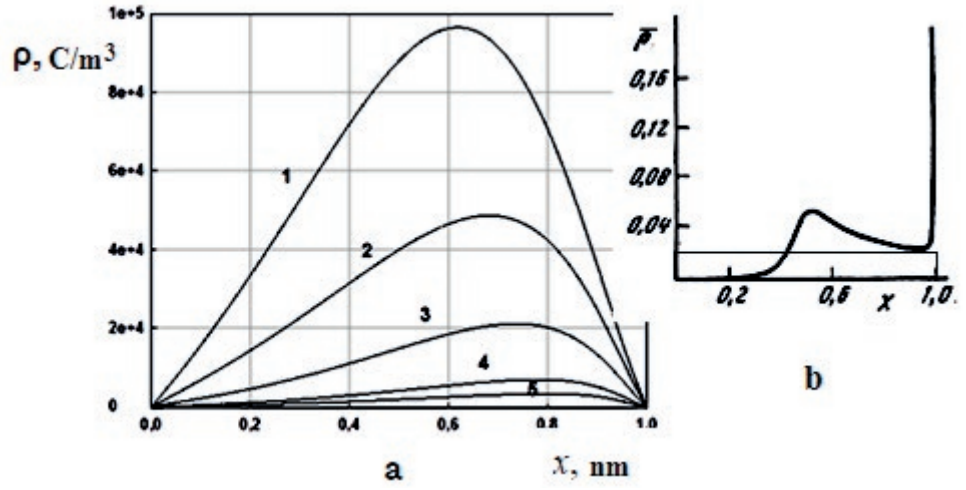

Fig. 4. Distribution of volumetric space charge ρ (C/m³) over the dimensionless coordinate of the layer at a thickness of: *1* – 10; *2* – 50; *3* – 100; *4* – 200; and *5* – 300 nm (a) and distribution of dimensionless charge density on dimensionless thickness of diffusion layer in the Rubinstein model [22, p. 325] (b)

by the boundary conditions of the problem set in study [21]. At the left and right boundaries of the layer, the electroneutrality condition is met. Therefore, the charge is zero at the boundary points $X = 0$ and $X = 1$. As the layer thickness increases, the maximum space charge decreases monotonically (Fig. 4a). The change of surface charge distribution over thickness of diffusion boundary layer according to the widely known Rubinstein model [22, p. 325] is shown in Fig. 4b. The mathematical models differ both by the approach to their description and by the studied objects. However, when the results were compared, we found that both models make it possible to estimate the space charge at the membrane surface and the size of the area of its localisation. It helped to better understand the mechanism of electroconvection in EMS.

The integral value of the dimensionless charge was approximately estimated as the area under the curve using the mean integral value (rectangle in Figure 4b). The conversion to a dimensional value provided the value: $\bar{\rho} = Fc_0\delta\int_0^L \rho \approx 0.002$ C/m², where F=10⁵ C/mol; $c_0 = 1$ mol/m³; and $\delta = 10^{-6}$ m.

The change in the integral value of the surface charge was not monotonic (Fig. 5). In the framework of the boundary value problem with electroneutrality conditions at the boundaries, the surface charge approaches zero as the layer thickness increases. The charge distribution over the layer thickness in the considered model corresponds to a thin boundary layer forming near the membrane in the Rubinstein model. We compared this value with the corresponding value at $x = 50$ nm (Fig. 5) and observed the same order of values (~0.0014 C/m²). The difference is that in the Rubinstein model the charge is distributed in a diffusion layer with a thickness of $(1–100)\cdot10^{-6}$ m, while in the presented model it is distributed at the interface in an area with a thickness of $(10–300)\cdot10^{-9}$ m. The thickness ratio is in the range of 10–1000.

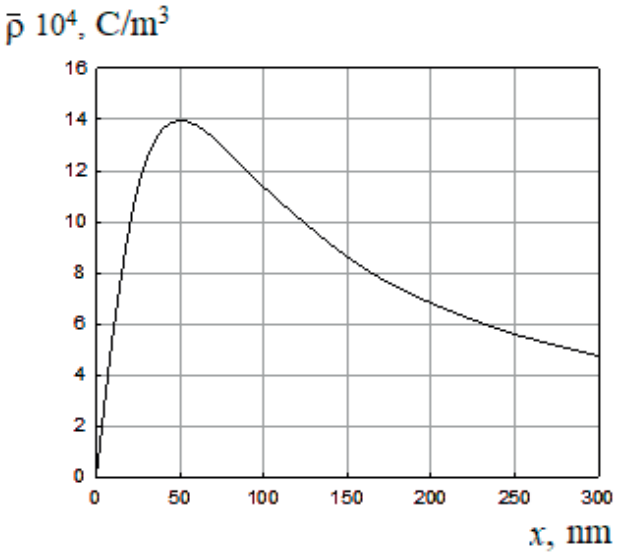

Fig. 5. Dependence of the dimensional integral surface charge density $\bar{\rho} = \int_0^L \rho dx$ on the layer thickness

It should be noted that both considered mathematical models do not provide entirely real values of size of the space charge distribution region. Spatial charge can be described more thoroughly, if the boundary value problem domain is extended beyond the height of the microprofile both towards the diffusion layer and towards the membrane phase region.

3. Results and discussion

Numerical calculations were performed under the condition of trapezoidal distribution of the body force (Fig. 1b) by formula (4) in accordance with characteristic structural parameters of the surface of real experimental ion-exchange membranes (Table 1). Fig. 6a shows the distribution of ion concentration near the surface of the cation-exchange membrane and the scheme of formation of two differently directed electroconvective vortices (*d* is the vortex diameter, δ is the diffusion layer thickness, λ is the SCR thickness, C'_{Na} and C'_{Cl} are the concentrations of counterions and coions in the solution, respectively, $\rho_{av} = \int_0^{\lambda} \rho(x)dx / \lambda$ is the mean integral charge density, and C_{Na} is the concentration of counterions in the SCR). Fig. 6b shows the results of numerical calculation of fluid flow lines in the section of membrane channel with heterogeneous membrane, where *y* is the horizontal coordinate, *x* is the vertical coordinate, L_3 and L_2 are the lengths of conductive (ion exchanger) and non-conductive (polyethylene) sections, respectively, and L_1 is the length of the transition sections.

We carried out two sequences of numerical calculations to determine the dependence of the size of electroconvective vortices on the current density for experimental membranes with different dimensions of conductive and non-conductive sections (Table 1). Taking into account the notations, the total length of conductive and non-conductive sections was ($L_0 = 2L_3 + L_2 + 4L_1$) 13.7 μm and 11.7 μm for membranes with mass fraction of ion exchange resin of 45 % and 70 %, respectively. Fig. 7 shows the distribution of fluid flow lines in the case when electroconvection occurs near both membranes, which form the desalting channel in the electrodialysis cell. When developing a two-dimensional mathematical model, we considered ion exchange membranes with only two conductive areas on the surface. The conductive sections are located in the middle part of the channel in order to avoid the influence of inlet and outlet boundary conditions of the

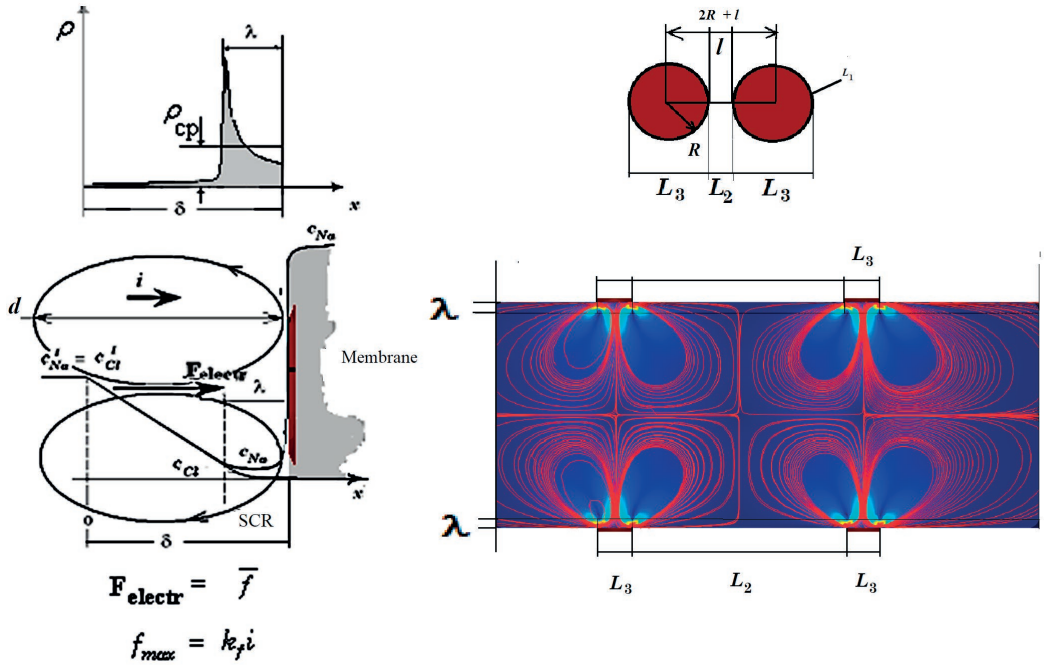

Fig. 6. The ion concentration distribution in the solution (a) and the pattern of the occurrence of electroconvective vortices (b) near the surface of heterogeneous cation-exchange membrane

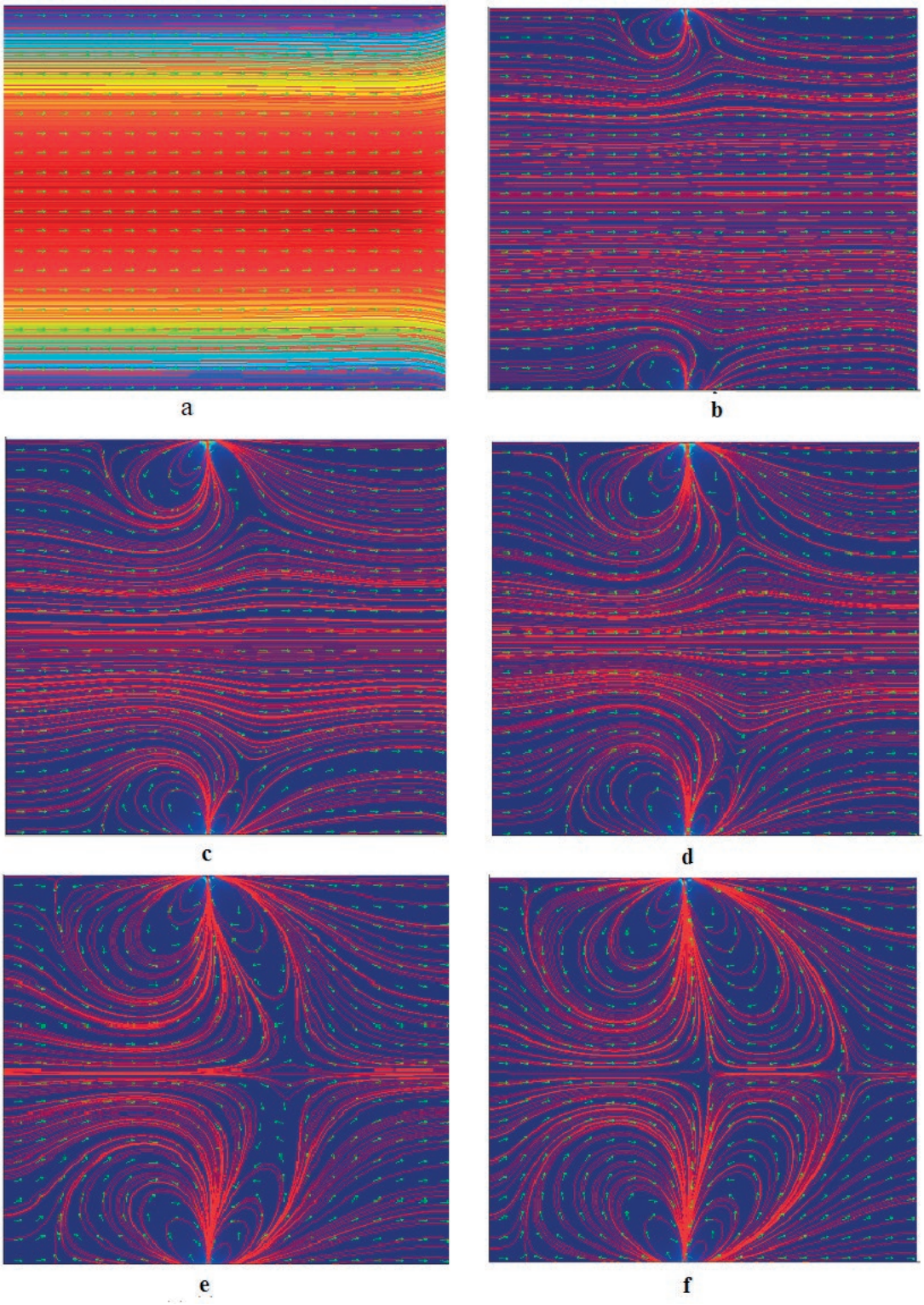

Fig. 7. Current lines and fluid flow velocity vectors in a membrane channel with two conductive sections on each of the membranes at different values exceeding the limiting current density i/i_{lim}: a – 1; b – 4; c – 8; d – 16, e – 32; and f – 64

channel. The rest of the membrane surface is inert (polyethylene). Numerical experiments with a sodium chloride solution showed that two vortices are formed near each membrane due to the heterogeneity of their surface (Fig. 7). The vortices are formed in front of the conductive section. In the case of the cation-exchange membrane, they rotate clockwise, and in the case of the anion-exchange membrane, the rotation is counterclockwise. At high current, the diameter of the vortices is commensurate with the channel width. It was determined that vortex structures arise with the onset of the limiting state, when, according to Rubinstein's theory, a space charge begins to form. The formation of four vortices was confirmed for membranes with large dimensions of surface inhomogeneity [10]. The total dimensions of the conductive and non-conductive sections of the studied membranes were, on average, an order of magnitude smaller. Therefore, the two internal vortices were almost invisible and had no effect on the external vortices. As the current density increases, the vortex sizes change nonlinearly and reach a value equal to half of the membrane channel thickness. Their further growth is limited by the size of the channel and the interaction of vortices on opposite membranes. The vortex diameter is considered to be the largest distance *d* between the points belonging to the area embraced by the closed current lines.

We assumed that the diameter *d* of the vortex at the membrane element (Fig. 1) depends on the magnitude of the electric force acting on the volume of the solution $F_{\max} = k_F \left(i - i_{\lim}\right)\delta$ according to nonlinear law [20]:

$$d\left(i\right) = \gamma_2 \left[F_{\max}\left(i\right)\right]^{\alpha} + \gamma_1 F_{0\max}\left(i\right) + \gamma_0, \quad (6)$$

where γ_i, α are the a priori numerical coefficients: γ_2, α are the coefficients taking into account the interaction of vortices; γ_1 is the coefficient of linear effect of electroconvection; and γ_0 is the coefficient considering other forces influencing the occurrence of vortices, besides the electric force. For current density not too much exceeding its limit value, there is no interaction of vortices. Therefore, formula (6) is simplified to $d\left(i\right) = \gamma_1 F_{\max} + \gamma_0$. In the dimensionless form, the formula is:

$$\frac{d}{H} = \overline{\gamma}_2 \left[I - 1\right]^{\alpha} + \overline{\gamma}_1 \left(I - 1\right) + \overline{\gamma}_0, \quad (7)$$

where $\overline{\gamma}_2$, $\overline{\gamma}_1$, $\overline{\gamma}_0$ are the dimensionless parameters:

$$\overline{\gamma}_2 = \frac{\gamma_2 k_F \delta^{\alpha} i_{\lim}^{0}}{H}, \ \overline{\gamma}_1 = \frac{\gamma_1 k_F \delta^{\alpha} i_{\lim}^{0}}{H}, \ \overline{\gamma}_0 = \frac{\gamma_0}{H}.$$

Formula (7) reveals the role of the dimensionless current parameter $I = \dfrac{i}{i_{\lim}}$ in the formation of vortex structures [17]. However, the size of the SCR is a more significant factor. In reality, alternating conductive and non-conductive sections are located along the entire length of the channel. The electric force acts on the space charge localised near the solution/membrane interface. If in this case $rot(f) = 0$, i.e. the vector field is potential (vortexless), the pressure changes evenly and no vortex motion occurs in the solution. On the other hand, the *rot*(*f*) value decreases as the proportion of conductive sections decreases. So, no vortex motion of the fluid can be observed in the case of a completely non-conductive surface. In both cases, the vortex diameter approaches zero. In intermediate cases, for the value of $rot(f) \neq 0$, there will be an extremum in the dependence of the size of electroconvective vortices on the ratio of surface inhomogeneities. The body force of electroconvection causes an uneven overpressure, which pushes the solution towards the membrane surface, but meets the resistance of the underlying fluid layers and the surface itself. This causes a change in the flow direction up to a complete reversal of the direction of fluid movement from the membrane surface to the depth of the solution. Oppositely directed currents form vortices, which partially destroy the diffusion layer and reduce the thickness of the charged layer. In turn, this leads to a decrease in the body force and, consequently, to a decrease in the vortex diameter.

We carried out numerical calculations of the dependence of the vortex diameters on current density for experimental heterogeneous sulphocation-exchange membranes with different ratios of conductive (L_3) and non-conductive (L_2) sections (Fig. 8). We also calculated the dependence of the vortex diameters on the length of non-conductive sections L_2 at different values of the body force, determining the

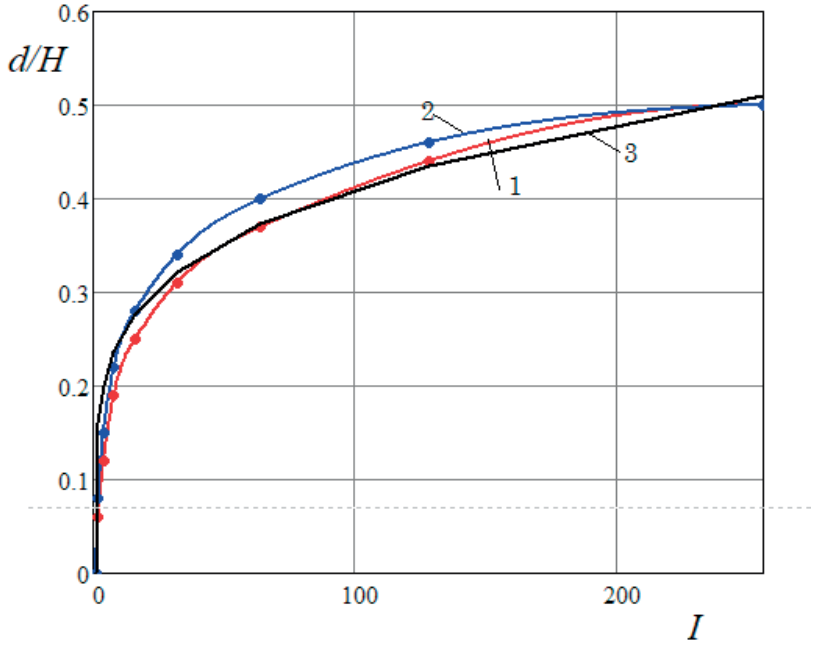

Fig. 8. Vortex diameter dependence on current at sulphocation-exchange membrane surface with the total size of conductive and non-conductive sections of $2L_3+L_2$ = 13.7 μm (*1*) and 11.7 μm (*2*) in the channel of an electrodialysis cell with a thickness of H = 2 mm at the Reynolds number Re = 2. *1*, *2* – numerical calculation, *3* – calculated by formula (9) at $\bar{\gamma}_2 = 0{,}16$; $\bar{\gamma}_1 = 10^{-4}$; $\bar{\gamma}_0 = 0$; $\alpha = 0.2$

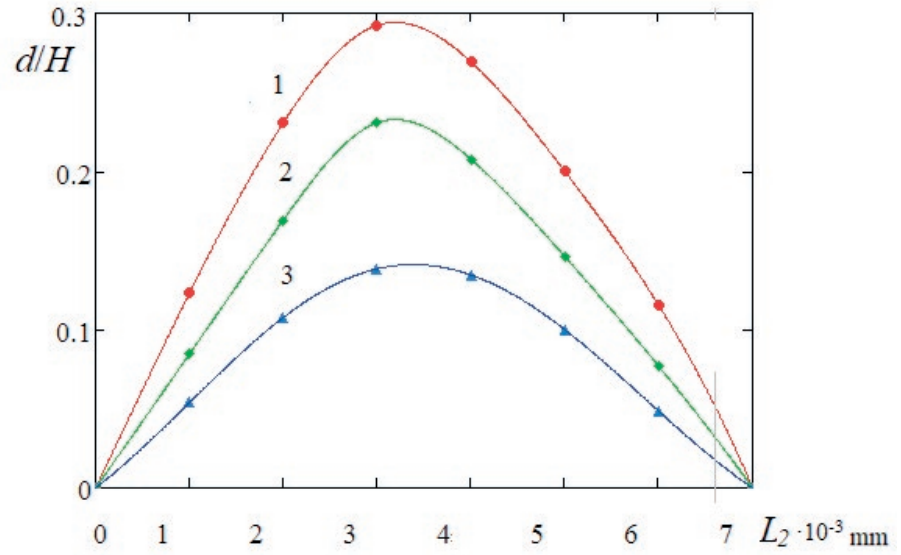

Fig. 9. Dimensionless dependence of vortex diameters on the channel width, as a function of the non-conductive section length L_2 at different values of the body force generating the rotor, 10^9 N/m^3: *1* – 4; *2* – 2; and *3* – 0.6

force rotor (Fig. 9). For this purpose, at a given total length of the section L_0, we changed the length of the conductive surface section L_3. The length of the non-conductive section L_2 was expressed by L_0 and L_3. We obtained the expression $L_2 = (L_0 - 2L_3 - 4L_1)/2$, where L_1 is the length of the transition region at the boundary between the conductive and non-conductive sections. The initial values of $\bar{L}_3 = 0.0046$ mm, $\bar{L}_2 = 0.0025$ mm, $\bar{L}_1 = 0.0001$ mm, and $L_0 = 0.0075$ mm were the experimentally found dimensions of the surface sections of the experimental membranes (Table 1). The minimum possible value of $L_{2\min} = (L_0 - 4L_1)/2$ corresponds to

the case of $L_3 = 0$, where there are no conductive sections on the surface. When modelling another marginal case with a decrease in L_2, the rotor of the body force decreased linearly according to the formula:

$$F = F_0 \cdot E_1(L_3), \quad (8)$$

where $E_1(L_3) = \begin{cases} \frac{L_3}{\bar{L}_3}, \text{if } L_3 \le \bar{L}_3 \\ 1, \text{if } L_3 \ge \bar{L}_3 \end{cases}$.

It was determined that under the conditions and approximations of the mathematical model, the vortex sizes reach their maximum value in the middle of the total length of the section L_0.

4. Conclusions

It was shown that the application of Rubinstein's theory of spatial charge together with the numerical modelling of ion transport phenomena using the Navier-Stokes hydrodynamic equations made it possible to conduct theoretical studies of convectively unstable structures in EMS. It was found that in the numerical modelling, the most important parameters are the size of the electrical heterogeneity sections of the membrane surface, the current density, and the length of the space charge region. The use of mathematical approaches allowed us to study the occurrence of electroconvective vortices at the membrane surface, including the study of the mutual influence of the vortices on each other.

We determined the fundamental correlations between the membrane surface morphology, electroconvection strength, and overlimiting mass transfer in electromembrane systems with different ion-exchange resin particle content. It was shown that an increase in the proportion of ion-exchange resin in the production of heterogeneous strongly acidic membranes promoted the formation and development of electroconvection in the membrane channel due to a decrease in the electrical inhomogeneity step of the surface.

The developed mathematical model of electroconvection in membrane channels with heterogeneous ion-exchange membranes may be a theoretical basis for targeted modification of their surface in order to develop new generation membranes. For these membranes, electroconvection will be the main mechanism of electrolyte ion transfer under intensive current modes.

Author contributions

All authors made an equivalent contribution to the preparation of the publication.

Conflict of interests

The authors declare that they have no known competing financial interests or personal relationships that could have influenced the work reported in this paper.

References

1. Zabolotskii V. I., Nikonenko V. V., Urtenov M. K., Lebedev K. A., Bugakov V. V. Electroconvection in systems with heterogeneous ion-exchange membranes. *Russian Journal of Electrochemistry*. 2012;48(7): 692–703. https://doi.org/10.1134/S102319351206016X

2. Zabolotsky V. I., Novak L., Kovalenko A. V., Nikonenko V. V., Urtenov M. Kh., Lebedev K. A., But A. Yu. Electroconvection in systems with heterogeneous ion-exchange membranes. *Petroleum Chemistry*. 2017;57(9): 779–789. https://doi.org/10.1134/S0965544117090109

3. Dukhin S. S., Mishchuk N. A. Intensification of electrodialysis based on electroosmosis of the second kind. *Journal of Membrane Science*. 1993;79(2-3): 199–210. https://doi.org/10.1016/0376-7388(93)85116-E

4. Mishchuk N. A. Electro-osmosis of the second kind near the heterogeneous ion-exchange membrane. *Colloids and Surfaces A: Physicochemical and Engineering Aspects*. 1998;140(1-3): 75–89. https://doi.org/10.1016/S0927-7757(98)00216-7

5. Rubinshtein I., Shtilman L. Voltage against current curves of cation-exchange membranes. *Journal of the Chemical Society, Faraday Transactions 2: Molecular and Chemical Physics*. 1979;75: 231–246. https://doi.org/10.1039/F29797500231

6. Rubinstein I., Zaltzman B., Kedem O. Electric fields in and around ion-exchange membranes. *Journal of Membrane Science*. 1997;125(1): 17–21. https://doi.org/10.1016/S0376-7388(96)00194-9

7. Rubinshtein I., Zaltsman B., Pretz I., Linder C. Experimental Verification of the electroosmotic mechanism of overlimiting conductance through a cation exchange electrodialysis membrane. *Russian Journal of Electrochemistry*. 2002;38: 853–863. https://doi.org/10.1023/A:1016861711744

8. Zabolotskii V. I., Loza S. A., Sharafan M. V. Physicochemical properties of profiled heterogeneous ion-exchange membranes. *Russian Journal of Electrochemistry*. 2005;41(10): 1053–1060. https://doi.org/10.1007/s11175-005-0180-2

9. Pis'menskaya N. D., Nikonenko V. V., Mel'Nik N. A., Pourcelli G., Larchet G. Effect of the

ion-exchange-membrane/solution interfacial characteristics on the mass transfer at severe current regimes. *Russian Journal of Electrochemistry*. 2012;48(6): 610–628. https://doi.org/10.1134/S1023193512060092

10. Zabolotsky V. I., Lebedev K. A., Vasilenko P. A., Kuzyakina M. V. Mathematical modeling of vortex structures during electroconvection in the channel of an electrodialyzer cell on model membranes with two conductive sections. *Ecological Bulletin of Scientific Centers of the Black Sea Economic Cooperation*. 2019;16(1): 73–82. (In Russ.) https://doi:10.31429/vestnik-16-1-73-82

11. Newman J. S. *Electrochemical systems*. New Jersey: Prentice-Hall, Inc., Englewood Cliffs; 1973. 432 p.

12. Roache P. J. *Computational fluid dynamics*. Hermosa Publishers; 1976. 446 p.

13. Vasil'eva V. I., Bityutskaya L. A., Zaichenko N. A. , Grechkina M. V., Botova T. S., Agapov B. L. Microscopic analysis of the surface morphology of ion-exchange membranes*. *Sorbtsionnye i Khromatograficheskie Protsessy*. 2008;8(2): 260-271. (In Russ.) http://www.chem.vsu.ru/sorbcr/images/pdf/20080210.pdf

14. Nikonenko V. V., Kovalenko A. V., Urtenov M. K., Pismenskaya N. D., Han J. Sistat P., Pourcelly G. Desalination at overlimiting currents: State-of-the-art and perspectives. *Desalination*. 2014;342: 85–106. https://doi.org/10.1016/j.desal.2014.01.008

15. Zabolotskii V. I., Lebedev K. A., Lovtsov E. G. Mathematical model for the overlimiting state of an ion-exchange membrane system. *Russian Journal of Electrochemistry*. 2006;48(2):836–846. https://doi.org/10.1134/S1023193506080052

16. Nikonenko V. V., Mareev S. A., Pis'menskaya N. D., Uzdenova A. M., Kovalenko A. V., Urtenov M. Kh., Pourcelly G. Effect of electroconvection and its use in intensifying the mass transfer in electrodialysis (Review). *Russian Journal of Electrochemistry*. 2017;53: 1122–1144. https://doi.org/10.1134/S1023193517090099

17. Rubinstein S. M., Manukyan G., Staicu A., Rubinstei I., Zaltzman B., Lammertink R. G. H., Mugele F., Wessling M. Direct observation of a nonequilibrium electro-osmotic instability. *Physical Review Letters*. 2008;101: 236101. https://doi.org/10.1103/PhysRevLett.101.236101

18. Urtenov M. Kh. *Boundary value problems for systems of nernst-planck-poisson equations (factorization, decomposition, models, numerical analysis)**. Krasnodar: KubGU Publ.; 1998. 126 p. (In Russ.)

19. Babeshko V. A., Zabolotskii V. I., Korzhenko N. M., Seidov R. R., Urtenov M. Kh. Stationary transport theory of binary electrolytes in the one-dimensional case: numerical analysis. *Doklady Physical Chemistry*. 1997;42(8): 836–846. Available at: https://www.elibrary.ru/item.asp?id=13268324

20. Zabolotskii V. I., Lebedev K. A., Urtenov M. K., Nikonenko V. V., Vasilenko P. A., Shaposhnik V. A., Vasil'eva V. I. A mathematical model describing voltammograms and transport numbers under intensive electrodialysis modes. *Russian Journal of Electrochemistry*. 2013;49(4). 369–380. https://doi.org/10.1134/S1023193513040149

21. Kasparov M. A., Lebedev K. A. Mathematical model of ion transport through the interface 'ion-exchange membrane / strong electrolyte'. *Ecological Bulletin of Scientific Centers of the Black Sea Economic Cooperation*. 2017;14(4-1): 40–49. (In Russ., abstract in Eng.). Available at: https://vestnik.kubsu.ru/article/view/756

22. Zabolotsky V. I., Nikonenko V. V. *Ion transport in membranes**. Moscow: Nauka Publ.; 1996. 392 p. (In Russ.)

23. Zabolotskiy V. I., But A. Yu., Vasil'eva V. I., Akberova E. M., Melnikov S. S. Ion transport and electrochemical stability of strongly basic anion-exchange membranes under high current electrodialysis conditions. *Journal of Membrane Science*. 2017;526: 60–72. https://doi.org/10.1016/j.memsci.2016.12.028

*Translated by author of the article.

Information about the authors

Konstantin A. Lebedev, Dr. Sci. (Phys.–Math.), Professor of the Department of Intellectual Information Systems, Kuban State University (Krasnodar, Russian Federation).

https://orcid.org/0000-0003-0950-9770
klebedev.ya@yandex.ru

Viktor I. Zabolotsky, Dr. Sci. (Chem.), Head of the Department of Physical Chemistry, Kuban State University (Krasnodar, Russian Federation).

https://orcid.org/0000-0002-9414-7307
vizab@chem.kubsu.ru

Vera I. Vasil'eva, Dr. Sci. (Chem.), Professor of the Department of Analytical Chemistry, Voronezh State University (Voronezh, Russian Federation).

https://orcid.org/0000-0003-2739-302X
viv155@mail.ru

Elmara M. Akberova, Cand. Sci. (Chem.), Leading Engineer of the Department of Analytical Chemistry, Voronezh State University (Voronezh, Russian Federation).

https://orcid.org/0000-0003-3461-7335
elmara_09@inbox.ru

Received 11.10.2021; approved after reviewing 07.11.2022; accepted for publication 15.11.2022; published online 25.12.2022.

Translated by Anastasiia Ananeva
Edited and proofread by Simon Cox